Inorg. Chem. **2007**, *46*, 1062–1070

Well-Defined Silica-Supported Rare-Earth Silylamides

Régis M. Gauvin,* Laurent Delevoye, Rahma Ali Hassan, Jérôme Keldenich, and André Mortreux

Unité de Catalyse et de Chimie du Solide UMR 8181 CNRS, ENSCL, BP 90108, 59652 Villeneuve d'Ascq Cedex, France

Received June 9, 2006

Rare-earth silylamides [Ln{N(SiMe$_3$)$_2$}$_3$] [**1a**–**d**, Ln = Y (**1a**), La (**1b**), Nd (**1c**), Sm (**1d**)] react with partially dehydroxylated silica to generate the singly surface-bonded species [(≡Si—O)Ln{N(SiMe$_3$)$_2$}$_2$] (**2a**–**d**). Trimethylsilylation of silanols occurs during the grafting process, affording in fine a hydroxyl-free surface. Contacting these well-defined surface species with excess triphenylphosphine oxide yields [(≡Si—O)Ln{N(SiMe$_3$)$_2$}$_2$(OPPh$_3$)] surface adducts **3a**–**d** as the major (80%) species, leaving about 20% of unreacted siloxide bisamido species (20%). In addition to elemental analysis and infrared spectroscopy, solid-state NMR spectroscopy was used to characterize these new materials and proved to be a particularly efficient tool for the study of the paramagnetic Nd- and Sm-containing materials and for providing unambiguous verification of OPPh$_3$ coordination on the rare-earth center. Silica-supported rare-earth amides **2a**–**d** are active catalysts for 1-hexene and styrene hydrosilylation and for phenylacetylene dimerization. When compared to the molecular species **1a**–**d**, grafting of the catalyst induces significant changes in the activity and selectivity of these systems.

Introduction

From the strategic importance of catalysis in environmental and economical issues stems a continuous demand for the generation of increasingly efficient catalysts. One of the approaches to meet this goal is the generation of heterogeneous catalysts with a controlled distribution of well-defined active sites.[1] Heterogeneization of (potential) molecular catalysts is considered to be a particularly promising approach to reach this objective.[2] Indeed, grafted catalysts should ideally combine the advantages of homogeneous catalysts (high activity and selectivity, tunable structure–activity relationship) with those of their heterogeneous counterparts (recycling, easy separation from reaction products, thermal robustness in the case of inorganic supports). Oxophilic early transition metals are prone to be directly grafted onto an oxide surface; indeed, the reaction of an organometallic or coordination compound with an inorganic oxide affords, if proper conditions are met, isolated metallic sites with a coordination sphere closely related to that of the molecular precursor.[3] These sites can, in turn, react further to yield highly reactive supported species. This so-called "surface organometallic chemistry" has experienced a considerable development by benefiting from the progress of the advanced spectroscopic methods currently available, which lead to better insight into the structure of the surface species.[4]

In recent years, lanthanide-based homogeneous catalysts have attracted growing attention. They have proven to be active in several fields, primarily in polymerization[5] and fine chemistry.[6] Among the various classes of compounds used as homogeneous catalysts or catalytic precursors, lanthanide amides have been found to be a most attractive and versatile family.[7] Recently, applications of supported rare-earth amido

* To whom correspondence should be addressed. E-mail: regis.gauvin@ensc-lille.fr. Fax: 00 33 3 2043 6585. Tel.: 00 33 3 2043 6754.

(1) Thomas, J. M.; Raja, R.; Lewis, D. W. *Angew. Chem., Int. Ed.* **2005**, *44*, 6456–6482.
(2) Louis, C.; Che, M. In *Preparation of Solid Catalysts*; Ertl, G., Knoezinger, H., Weitkamp, J., Eds.; Wiley-VCH Verlag, Weinheim, Germany, 1999; pp 341–355.
(3) (a) Ermakov, Y. I. *J. Mol. Catal.* **1983**, *21*, 35–55. (b) Basset, J.-M.; Choplin, A. *J. Mol. Catal.* **1983**, *21*, 95–108. (c) Marks, T. J. *Acc. Chem. Res.* **1992**, *25*, 57–65.
(4) Copéret, C.; Chabanas, M.; Petroff Saint-Arroman, R.; Basset, J.-M. *Angew. Chem., Int. Ed.* **2003**, *42*, 156–181.
(5) Gromada, J.; Carpentier, J.-F.; Mortreux, A. *Coord. Chem. Rev.* **2004**, *248*, 397–410.
(6) (a) Mikami, K.; Terada, M.; Matsuzawa, H. *Angew. Chem., Int. Ed.* **2002**, *41*, 3554–3572. (b) Molander, G. A.; Romero, J. A. C. *Chem. Rev.* **2002**, *102*, 2161–2186. (c) Shibasaki, M.; Yoshikawa, N. *Chem. Rev.* **2002**, *102*, 2187–2210. (d) Inanaga, J.; Furuno, H.; Hayano, T. *Chem. Rev.* **2002**, *102*, 2211–2226. (e) Kobayashi, S.; Sugiura, M.; Kitagawa, H.; Lam, W. W.-L. *Chem. Rev.* **2002**, *102*, 2227–2302.

10.1021/ic0610334 CCC: $37.00
Published on Web 01/24/2007

(pre)catalysts have been reported.[8] As demonstrated in the pioneering work of Anwander and collaborators, lanthanide (extended) silylamide complexes can be grafted onto (mesoporous) silica, yielding surface lanthanide amido complexes that can be subjected to further ligand-sphere modifications to generate materials that are catalytically active in a broad variety of reactions.[8c,9] However, analyses of the surface species distribution revealed the concomitant presence of mono- and bipodal surface lanthanide species, a situation that can be detrimental to the properties of such materials in terms of catalytic selectivity and further ligand-sphere modifications. Recently, we reported that convenient treatment of the inorganic silica support affords selective formation of monografted lanthanide bisamides and that surface species distribution (mono- vs bigrafted) has a direct influence on the activity and selectivity of a lanthanum-based system in methyl methacrylate polymerization.[10] Along these lines, we embarked on the synthesis and study of a family of well-defined supported rare-earth amides. We present here our results concerning the grafting of yttrium, lanthanum, neodymium, and samarium trisamides onto dehydroxylated silica; their reactivity toward a molecular probe, triphenylphosphine oxide; and studies on their catalytic performances in alkene hydrosilylation and alkyne dimerization.[11]

Experimental Section

General Considerations. Manipulations were carried out under an argon atmosphere in an M-Braun glovebox or using Schlenk techniques. Lanthanide chlorides were purchased from Strem Chemicals. Triphenylphosphine oxide (Aldrich) was dried under secondary vacuum (10^{-6} mmHg). Solvents, hexene, and phenylsilane were dried using conventional reagents and stored in a glovebox over 3A molecular sieves. Styrene and phenylacetylene were dried over conventional reagents and distilled shortly before use. Rare-earth silylamides were prepared by following literature procedures.[12] Liquid-state NMR analyses were run on a Bruker Avance 300 spectrometer. Solid-state MAS NMR spectra were recorded on a Bruker Avance 400 spectrometer (^{1}H, 400.1 MHz; ^{13}C, 100.6 MHz; ^{29}Si, 79.5 MHz; ^{31}P, 161.2 MHz). For ^{1}H experiments, the spinning frequency was 20 kHz, the recycle delay was 5 s, and 64 scans were collected using a 90° pulse excitation of 3 μs. The two-dimensional homonuclear experiment (DQ-MAS) was performed using excitation and reconversion pulse blocks of two rotor periods each (100 μs), at a spinning frequency of 20 kHz. The 90° pulse length was 3 μs, the recycle delay was 5 s, and 16 scans were collected. For the ^{29}Si CP experiment, the spinning frequency was 6 kHz, the recycle delay was 5 s, and 16384 scans were collected. The ^{1}H−^{13}C CP experiments were performed at a spinning frequency of 10 kHz, with a recycle delay of 5 s and collection of 1024 scans. For the CP step, a ramped radio-frequency (RF) field centered at 50 kHz was applied on protons, whereas the silicon (or carbon) RF field was matched to obtain optimal signal. The contact time was set to 8 and 1.5 ms for ^{29}Si and ^{13}C CP experiments, respectively. The ^{31}P spectra were acquired at a spinning frequency of 14 kHz, with a recycle delay of 30 s and collection of 64 scans. During acquisition, the proton decoupling field strength was set to 83 kHz. Chemical shifts are reported with respect to TMS, and phosphoric acid (80%) as external references for ^{1}H−^{13}C−^{29}Si and ^{31}P NMR spectra, respectively. Diffuse reflectance infrared spectra were collected using a Harrick cell on a Nicolet Avatar spectrometer fitted with a MCT detector. Elemental analyses were carried out at the Service Central d'Analyse du CNRS (metals and phosphorus) and at the Service d'Analyse Elémentaire, LSEO, Université de Bourgogne (C, H, N). Gas chromatography analyses were performed on a Chrompack CP9001 gas chromatograph under N_2 flow with a CPSil 8 CB column (15-m length, 0.32-mm diameter, 0.25-μm film thickness). Aerosil 380 silica (Degussa, specific area 380 $m^2\ g^{-1}$, prior to heat treatment) was subjected to heating under secondary vacuum (10^{-6} mmHg) for 15 h at 500 °C, followed by 4 h at 700 °C, and stored in a glovebox.

Typical Synthesis of 2a−d. In a glovebox, a double-Schlenk apparatus was loaded with the chosen molecular precursor **1a** (570 mg, 1 mmol) dissolved in 10 mL of toluene in one compartment and with silica dehydroxylated at 700 °C (1 g) suspended in 10 mL of toluene in the other compartment. The complex solution was added to the support by filtering through the sintered glass separating the two Schlenk tubes, and the reaction mixture was stirred for 15 h at room temperature. The supernatant liquid was then separated by filtration into the other compartment, from which toluene was gas-phase transferred by trap-to-trap distillation back into the compartment containing the modified support in order to wash away the residual molecular precursor. This operation was repeated twice. The resulting white powder **2a** was then dried under secondary vacuum (10^{-6} mmHg) at 80 °C for 6 h.

Alcoholysis of **2a−d** to quantify Ln-{$N(SiMe_3)_2$} moieties was carried out by adding 0.70 mL of a stock solution of ^{t}BuOH (0.1 mol L^{-1}) and mesitylene (0.1 mol L^{-1}) in toluene to a suspension of 100 mg of the considered material (**2a−d**) in 2 mL of toluene and immediately determining the quantity of released hexamethyldisilazane by gas chromatography using mesitylene as the internal standard.

Typical Synthesis of 3a−d. To a suspension of **2a** (225 mg, 63 μmol of Y) in 10 mL of toluene was added dropwise a solution of 3 equiv per metal of triphenylphosphine oxide (53 mg, 189 μmol). After 1 h of stirring at room temperature, the modified silica was allowed to settle, and the supernatant was decanted off. After successive washings with two 10-mL portions of toluene and two 10-mL portions of pentane, the resulting white solid **3a** was dried under secondary vacuum (10^{-6} mmHg) at room temperature for 6 h.

(7) (a) Giardello, M. A.; Yamamoto, Y.; Brard, L.; Marks, T. J. *J. Am. Chem. Soc.* **1995**, *117*, 3276−3277. (b) Berberich, H.; Roesky, P. W. *Angew. Chem., Int. Ed.* **1998**, *37*, 1569−1571. (c) Kim, Y. K.; Livinghouse, T.; Bercaw, J. E. *Tetrahedron Lett.* **2001**, *42*, 2933−2935. (d) Kim, Y. K.; Livinghouse, T. *Angew. Chem., Int. Ed.* **2002**, *41*, 3645−3647. (e) Gribkov, D. V.; Hultzsch, K. C.; Hampel, F. *Chem. Eur. J.* **2003**, *9*, 4796−4810. (f) Kawaoka, A. M.; Douglass, M. R.; Marks, T. J. *Organometallics* **2003**, *22*, 4630−4632. (g) Suzuki, M.; Kata, N.; Kanai, M.; Shibasaki, M. *Org. Lett.* **2005**, *7*, 2527−2530. (h) Chen, Y.; Zhu, Z.;Zhang, J.; Shena, J.; Zhou, X. *J. Organomet. Chem.* **2005**, *690*, 3783−3789.

(8) (a) Woodman, T. J.; Sarazin, Y.; Fink, G.; Hauschild, K.; Bochmann, M. *Macromolecules* **2005**, *38*, 3060−3067. (b) Tortosa, K.; Hamaide, T.; Boisson, C.; Spitz, R. *Macromol. Chem. Phys.* **2001**, *2*, 1156−1160. (c) Gerstberger, G.; Palm, C.; Anwander, R. *Chem. Eur. J.* **1999**, *5*, 997−1005. (d) Gerstberger, G.; Anwander, R. *Microporous Mesoporous Mater.* **2001**, *44*−*45*, 303−310.

(9) (a) Anwander, R.; Roesky, R. *J. Chem. Soc., Dalton Trans.* **1997**, 137−138. (b) Anwander, R.; Runte, O.; Eppinger, J.; Gestberger, G.; Herdtweck, E.; Spiegler, M. *J. Chem. Soc., Dalton Trans.* **1998**, 847−858. (c) Nagl, I.; Widenmeyer, M.; Herdtweck, E.; Raudaschl-Sieber, G.; Anwander, R. *Microporous Mesoporous Mater.* **2001**, *44*−*45*, 311−319. (d) Liang, Y.; Anwander, R. *Dalton Trans.* **2006**, 1909−1918.

(10) Gauvin, R. M.; Mortreux, A. *Chem. Commun.* **2005**, 1146−1148.

(11) Some of these results have been communicated; see ref 10.

(12) (a) Bradley, D. C.; Ghotra, J. S.; Hart, F. A. *J. Chem. Soc., Chem. Commun.* **1972**, *6*, 349−350. (b) Bradley, D. C.; Ghotra, J. S.; Hart, F. A. *J. Chem. Soc., Dalton Trans.* **1973**, 1021−1023.

Typical Hydrosilylation Reaction. In a sealeable vial, a solution of 130 mg of phenylsilane (1.2 mmol) and 96 mg of 1-hexene (1.1 mmol) in 0.5 mL of toluene was added to a suspension of 105 mg of **2b** (28 μmol of La) in 1 mL of toluene. The reaction mixture is stirred at 60 °C. The suspended solid gradually turned to yellow, whereas the supernatant liquid remained colorless. After 15 h of reaction, the liquid phase was separated by filtration and washed with three 1-mL toluene portions. After evaporation to dryness, 207 mg of a colorless oil were obtained (98% yield). The regioselectivity of silane addition was measured by NMR spectroscopy.[31b]

Typical Alkyne Dimerization Reaction. In a sealeable vial, a solution of 140 mg of phenylacetylene (1.37 mmol) in 3 mL of toluene was added to a suspension of 105 mg of **2b** (28 μmol of La) in 2 mL of toluene. The reaction mixture was heated at 100 °C for 15 h. The suspended solid gradually turned brown-orange, whereas the supernatant liquid was pale orange. After the mixture had cooled to room temperature, the liquid phase was separated by filtration and washed with three 1-mL toluene portions. Mesitylene (63.5 mg) was then added as an internal standard, and the reaction mixture was injected into a gas chromatograph to determine the conversion of phenylacetylene and the selectivity toward **8**−**10**. The reaction mixture was then evaporated under vaccum to afford an orange oil. The yields of dimerization products **8**−**10** were determined by ^{1}H NMR spectroscopy by using ferrocene (6.1 mg) as an internal standard. Selectivities toward known compounds **8**−**10** were confirmed by ^{1}H NMR spectroscopy.[13]

Results and Discussion

1. Reaction of [Ln{N(SiMe$_3$)$_2$}$_3$] (1a−d) with Dehydroxylated Silica. a. Synthesis and Elemental Analysis Data of the Grafted Amides 2a−d. The selected rare-earth amide molecular precursors are the homoleptic derivatives of the type [Ln{N(SiMe$_3$)$_2$}$_3$] [Ln = Y (**1a**), La (**1b**), Nd (**1c**), Sm (**1d**)], originally described by Bradley and coworkers.[12] These complexes present promising features for their controlled grafting onto inorganic supports: Their monomeric structure can afford monometallic surface species, and their coordination sphere, devoid of additional donor ligand, can induce, upon grafting, coordinative unsaturation in the generated supported species and, therefore, afford high reactivity. As shown by Anwander et al., these compounds react with silica's hydroxyl groups, generating a covalent lanthanide−siloxide bond by protonolysis of the lanthanide−amido bond.[9] This reaction pattern is closely related to the alcoholysis of lanthanide amido species in solution, a well-known entry to alkoxo derivatives.[14] The released hexamethyldisilazane also reacts with the ≡Si−OH functionality to form ≡Si−O−SiMe$_3$ groups and, in fine, NH$_3$ via transient NH$_2$(SiMe$_3$).[15]

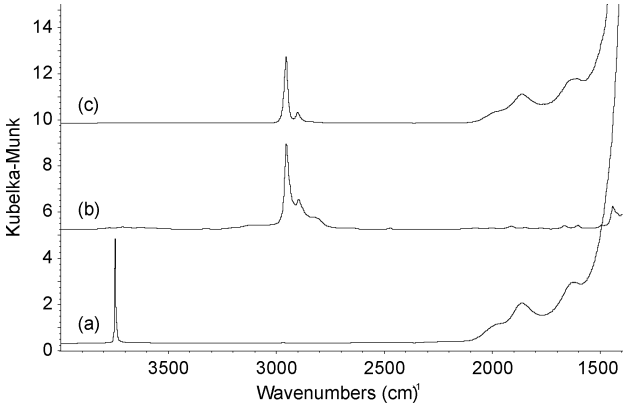

Figure 1. DRIFT spectra of starting dehydrated (a) silica, (b) **1a**, and (c) **2a**.

Scheme 1. Synthesis of Grafted Rare-Earth Silylamides **2a**−**d**

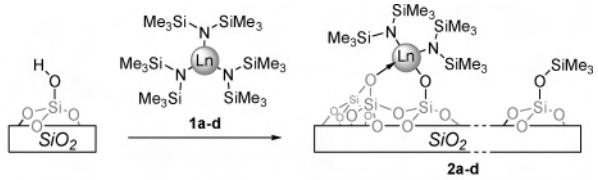

The chosen support, a nonporous flame silica (Aerosil 380, Degussa, 380 m^2 g^{-1}) was pretreated at 700 °C under vacuum (10^{-6} mmHg) to generate a silica surface presenting a single silanol type, namely, isolated silanols.[16] This is apparent in its DRIFT (diffuse reflectance infrared Fourier transform) spectrum (Figure 1a), where the stretching O−H band appears at 3747 cm^{-1}. The surface silanol content was determined by titration with dibenzylmagnesium[17] to be 0.62 mmol g^{-1} (1.10 OH nm^{-2}).

Grafting of the lanthanide amides onto silica was carried out at room temperature in toluene under inert conditions (see Scheme 1). Unreacted excess molecular precursor was separated from the modified support by three successive toluene washings. Subsequent evacuation of the volatiles under secondary vacuum (10^{-6} mmHg) at 80 °C afforded modified silicas **2a**−**d** as free-flowing colorless (**2a**, **2b**, **2d**) or light blue (**2c**) powders. In addition to unreacted lanthanide starting material, NMR and GC analyses of the washing fractions revealed the presence of hexamethyldisilazane, as expected from the postulated reaction scheme.

Similar metal loadings were obtained for the modified silicas **2a**−**d**: about 0.28 mmol of rare-earth metal was grafted per gram of material, which is consistent with similar surface chemistry over the rare-earth series studied here. Moreover, elemental analyses of **2a**−**d** indicate a N/Ln molar ratio of close to 2, which confirms the selective formation of monografted bisamido species of the type [(≡Si−O)Ln{N(SiMe$_3$)$_2$}$_2$] (Table 1).

To further confirm the stoichiometry of the grafting reaction, alcoholysis of the metal−amide bonds of **2a,b** by excess *tert*-butanol was performed. The released hexameth-

(13) (a) Yi, C. S.; Liu, N. *Organometallics* **1996**, *15*, 3968−3971. (b) Trost, B. M.; Sorum, M. T.; Chan, C.; Harms, A. E.; Rühter, G. *J. Am. Chem. Soc.* **1997**, *119*, 698−708.
(14) (a) Hitchcock, P. B.; Lappert, M. F.; Singh, A. *J. Chem. Soc., Chem. Commun.* **1983**, 1499−1501. (b) Stechner, H. A.; Sen, A.; Rheingold, A. L. *Inorg. Chem.* **1989**, *28*, 3280−3282. (c) Bradley, D. C.; Chudzynska, H.; Hursthouse, M. B.; Motavelli, M. *Polyhedron*, **1991**, *10*, 1049−1059. (d) Gromada, J.; Mortreux, A.; Chenal, T.; Ziller, J. W.; Leising, F.; Carpentier, J.-F. *Chem. Eur. J.* **2002**, *8*, 3773−3788.
(15) (a) Impens, N. R. E. N.; van der Voort, P.; Vansant, E. F. *Microporous Mesoporous Mater.* **1999**, *28*, 217−232. (b) Hertl, W.; Hair, M. L. *J. Phys. Chem.* **1971**, *75*, 2181−2185. (c) Windorf, D. W.; Maciel, G. E. *J. Phys. Chem.* **1982**, *86*, 5208−5219.
(16) McDonald, R. S. *J. Phys. Chem.* **1958**, *62*, 1168−1178.
(17) Fujdala, K. L.; Tilley, T. D. *J. Am. Chem. Soc.* **2001**, *123*, 10133−10134.

Table 1. Elemental Analysis Data for **2a**−**d** [Ln = Y (**2a**), La (**2b**), Nd (**2c**), Sm (**2d**)]

	Ln (wt %)	Ln (mmol g^{-1})	N (wt %)	N/Ln (mol/mol)	C (wt %)	H (wt %)
2a	2.47	0.278	0.80	2.06	4.54	1.06
2b	3.80	0.274	0.80	2.09	4.60	1.10
2c	4.12	0.286	0.79	1.98	4.65	1.10
2d	4.27	0.284	0.80	2.02	4.55	1.08

yldisilazane was quantified by GC analysis, using mesitylene as an internal standard. The values of released amine per rare-earth center (**2a**, 1.97; **2b**, 1.95; **2c**, 2.01; **2d**, 1.93 mol/mol) are consistent with two amido ligands per metal center and thus with the formulation of the surface species as [(≡Si−O)Ln{$N(SiMe_3)_2$}$_2$].

b. DRIFTS Studies on 2a−d. The infrared spectroscopic features of modified silicas **2a**−**d** are similar. The spectrum of yttrium-derivatized **2a** is presented in Figure 1. Complete consumption of the surface silanols occurred during the grafting process, as evidenced by the disappearance of the ν_{OH} signal at 3747 cm^{-1} in the starting spectrum of silica (Figure 1). Traces of residual silanols are observed as a very weak broad peak centered around 3710 cm^{-1}. The appearance of ν_{C-H} bands at 2955 and 2901 cm^{-1}, with a shoulder centered around 2820 cm^{-1}, is indicative of the introduction of $SiMe_3$ groups on the surface, as Ln−$N(SiMe_3)_2$ moieties and ≡Si−O−$SiMe_3$ groups. These values are slightly shifted compared to those of the molecular precursor **1a** (2954, 2897, and 2829 cm^{-1}; Figure 1b).

No ν_{N-H} signal was detected in the spectra of the isolated materials after treatment under high vacuum (10^{-6} mmHg, 80 °C, 6 h). However, when the modified silica was merely subjected to primary vacuum (10^{-2} mmHg, 25 °C, 6 h), bands resulting from N−H vibrations were observed as a broad peak centered around 3380 cm^{-1} with a shoulder around 3320 cm^{-1} (Figure 2a). Moreover, the signals in the ν_{C-H} region were significantly modified, as new overlapping peaks were observed at 2984 and 2888 cm^{-1}. After the material had been dried at 80 °C under secondary vacuum (10^{-6} mmHg), the spectrum became simplified, as the N−H peaks and the extra ν_{C-H} signals disappeared. Because coordination of the bulky amines $HN(SiMe_3)_2$ and $H_2N(SiMe_3)$ is unlikely in such a sterically crowded environment, and on the basis of Anwander et al.'s previous results on similar systems, we assigned these observations to the partial formation of an adduct, [(≡Si−O)Ln{$N(SiMe_3)_2$}$_2$(NH_3)$_n$]. As mentioned above, ammonia originates from the reaction of $HN(SiMe_3)_2$ with surface silanol groups. Coordinated ammonia gives rise to two N−H elongation bands, corresponding to asymmetric and symmetric vibration modes,[9b,18] and has a significant effect on the $SiMe_3$ moieties, as evidenced by the distinct ν_{C-H} signals. This adduct releases NH_3 upon heating under high vacuum, thus generating the donor-free [(≡Si−O)Ln{$N(SiMe_3)_2$}$_2$] surface complex. This reaction pattern is reminiscent of Wolczanski et al.'s isolation of the [Sc{$OSi(^tBu)_3$}$_3$(NH_3)] ammonia adduct from the alcoholysis of [Sc{$N(SiMe_3)_2$}$_3$] by excess $^tBu_3SiOH$.[19] However, in the case of this trissiloxy compound, ammonia dissociation could not be achieved by heating in vacuo.

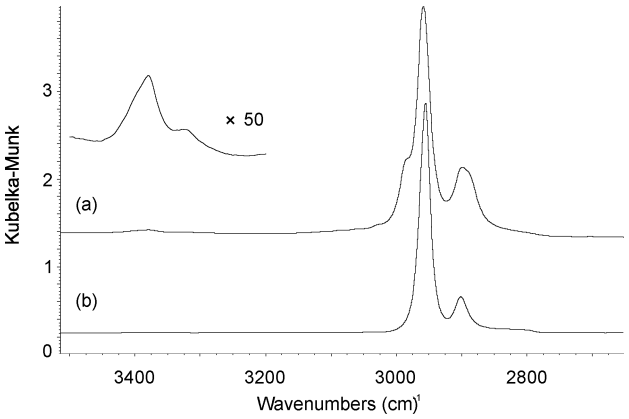

Figure 2. DRIFT spectra of **2a** (a) before and (b) after treatment at 80 °C under vacuum (10^{-6} mmHg).

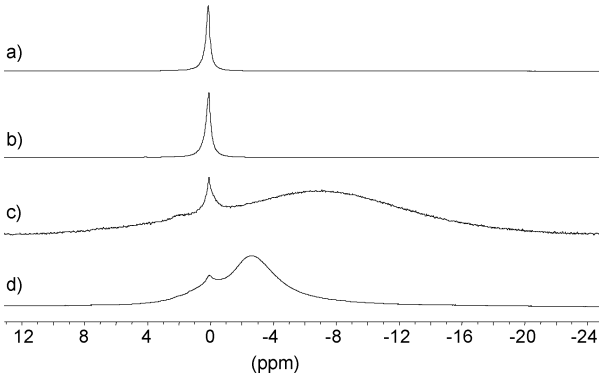

Figure 3. ^{1}H MAS spectra of (a) **2a**, (b) **2b**, (c) **2c**, and (d) **2d** (400 MHz).

c. MAS NMR Studies on 2a−d. ^{1}H MAS NMR studies on the **2a**−**d** family proved to be particularly informative, as some of the synthesized materials, namely, those containing Nd and Sm, have a paramagnetic character that induces a significant shift in the signal of the bis(trimethyl)silylamido protons. As expected, the ^{1}H NMR spectra of the yttrium- (**2a**) and lanthanum- (**2b**) grafted silicas each exhibit a single peak centered at 0.13 ppm ($\Delta\nu_{1/2}$ = 140 Hz) and 0.09 ppm ($\Delta\nu_{1/2}$ = 120 Hz), respectively, accounting for the undifferentiated Ln−$N(SiMe_3)$ and −O−$SiMe_3$ protons (Figure 3). On the other hand, the NMR spectra of **2c** and **2d** comprise a broad signal centered at −7.1 ppm ($\Delta\nu_{1/2}$ = 5600 Hz) and −2.6 ppm ($\Delta\nu_{1/2}$ = 2000 Hz), respectively, in addition to the unperturbed signal of the ≡Si−O−$SiMe_3$ group at 0.1 ppm (Figure 3).[20] As a comparison, the protons of molecular precursors [Nd{$N(SiMe_3)_2$}$_3$] (**1c**) and [Sm{$N(SiMe_3)_2$}$_3$] (**1d**) resonate at −6.26 and −1.49 ppm, respectively. Thus, in the case of these two latter complexes, a paramagnetic shift allows clear spectroscopic distinction between silylated silanols (≡Si−O−$SiMe_3$) and silylamido groups [Ln−$N(SiMe_3)_2$].

(18) We exclude the assignment of these bands to the formation of ≡Si−O−NH_2 groups resulting from NH_3 chemisorption (reaction with strained ≡Si−O−Si≡ bridges), because these groups yield bands at 3526 and 3446 cm^{-1}: (a) Peri, J. B. *J. Phys. Chem.* **1966**, *70*, 2937−2945. (b) Morrow, B. A.; Coody, I. A.; Lee, L. S. M. *J. Phys. Chem.* **1976**, *80*, 2761−2767.

(19) Covert, K. J.; Neithamer, D. R.; Zonnevylle, M. C.; LaPointe, R. E.; Schaller, C. P.; Wolczanski, P. T. *Inorg. Chem.* **1991**, *30*, 2494−2508.

(20) Haukka, S.; Root, A. *J. Phys. Chem.* **1994**, *98*, 1695−1703.

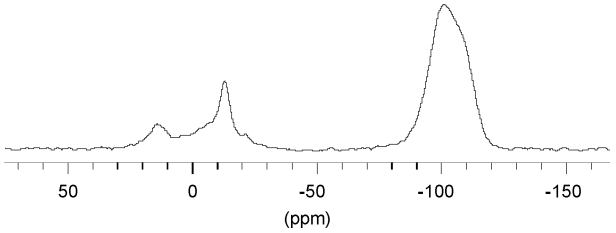

Figure 4. ^{29}Si CP-MAS spectrum of **2a** (79.5 MHz).

The ^{29}Si CP-MAS NMR spectrum of **2a** shows, in addition to the expected SiO_2 signal at −110 ppm, two sharp peaks centered at −13.1 and 13.9 ppm (Figure 4). The former can be assigned to grafted yttrium silylamides, bearing in mind the ^{29}Si chemical shift of the molecular precursor at −11.14 ppm (C_6D_6), and the latter corresponds to silylated hydroxyl groups, ≡Si−O−$SiMe_3$.[20] This confirms the concomitant presence of the two types of trimethylsilyl groups on the modified silica that could not be distinguished by either ^{1}H or ^{13}C MAS NMR spectroscopy in the case of diamagnetic lanthanides. Attempts to record the ^{89}Y CP-MAS NMR spectrum of **2a** following the procedure described by Wu and Evans[21] were not successful, most probably because of the lack of efficient magnetization transfer between the grafted species' protons and the ^{89}Y center, even using mixing times up to 20 ms.

d. Discussion. The low metal loadings of 0.28 mmol g^{-1} indicate that only one-half of the available silanols (0.62 mmol g^{-1}) have been metalated. Instead of the expected maximum lanthanide atom surface density of 1.09 nm^{-2}, this corresponds to a surface density of 0.49 nm^{-2}, which implies a surface interatomic average distance of about 1.6 nm. Simple molecular modeling hints at a radius of surface occupancy of about 6 Å, from which a maximum density of 0.7 nm^{-2} can be estimated. The complete disappearance of the ≡Si−OH group of silica implies that the silanols that have not been metalated have been transformed into ≡Si−O−$SiMe_3$ groups. The two types of sites can be spectroscopically distinguished by ^{29}Si MAS NMR spectroscopy, as well as by ^{1}H NMR spectroscopy in the case of paramagnetic materials. The side reaction of surface silanols with hexamethyldisilazane released during the grafting process thus consumes some of the available OH groups that could have reacted with the metallic precursor. The capping of residual silanols by $SiMe_3$ groups has been shown to considerably affect the reactivity and selectivity of supported catalysts, by preventing silanol-induced poisoning reactions or by modifying the hydrophobic/hydrophilic character of the surface.[8c,22]

Alcoholysis performed on supported rare-earth amides leads to the release of 2 equiv of hexamethyldisilazane per metal center. Combined with the elemental analysis results, which indicate a nitrogen-to-rare-earth ratio of 2, this confirms the formulation of the grafted species as a monosiloxibisamido surface compound. The presence of residual physisorbed species that would modify the N/Ln ratio is ruled out because these species are washed away during the workup procedure. This is particularly apparent in the case of the synthesis of **2c**: The blue-colored precursor **1c** is extracted from the solid by the successive washings, with the coloration of the toluene extracts evolving from light blue for the first extraction to colorless for the third. Another possible factor perturbing the N/Ln ratio, namely, the presence of residual ammonia bound to the metal center, is ruled out because the expected bands are not observed in the DRIFT spectra of materials **2a**−**d**.

Even though the nature and number of anionic ligands of the grafted species can be determined, the presence of an additional donor function originating from the support cannot be addressed spectroscopically. Previous surface organometallic chemistry studies have shown that surface siloxane bridges can interact strongly with grafted electrophilic metal centers.[4] Indeed, in the surface species considered in the present study, both the low coordination number (two amides and a siloxide as anionic ligands) and the highly oxophilic nature of the lanthanide metals[23] render highly probable the existence of an interaction with a neighboring bridging oxygen from a surface siloxane group. The study of the reaction of materials **2a**−**d** with a Lewis base might thus prove to be of interest in probing the strength of this dative bond.

Table 2. Elemental Analysis Data for **3a**−**d** [Ln = Y (**3a**), La (**3b**), Nd (**3c**), Sm (**3d**)]

	Ln (wt %)	P (wt %)	P/Ln (mol/mol)
3a	2.35	0.68	0.83
3b	3.62	0.63	0.78
3c	3.84	0.65	0.79
3d	4.06	0.67	0.80

Scheme 2. Reaction of Grafted Rare-Earth Silylamides **2a**−**d** with Triphenylphosphine Oxide

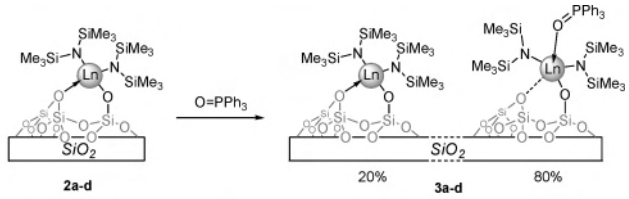

Ln = Y(**a**), La (**b**), Nd (**c**), Sm (**d**)

2. Reaction of [(≡Si−O)Ln{N(SiMe$_3$)$_2$}$_2$] (2a−d) with Triphenylphosphine Oxide. a. Synthesis and Elemental Analysis Data of 3a−d. Rare-earth hexamethyldisilylamides [Ln{N(SiMe$_3$)$_2$}$_3$] are known to react with triphenylphosphine oxide to afford monoadducts [Ln{N(SiMe$_3$)$_2$}$_3$(O=PPh$_3$)].[24a] The coordination of the $OPPh_3$ ligand is reversible: $OPPh_3$ sublimes away upon heating under vacuum. This

(21) Wu, J.; Boyle, T. J.; Shreeve, J. L.; Ziller, J. W.; Evans, W. *J. Inorg. Chem.* **1993**, *32*, 1130−1134.

(22) For selected examples, see: (a) Cauvel, A.; Renard, G.; Brunel, D. *J. Org. Chem.* **1997**, *62*, 749−752. (b) D'Amore, M. B.; Schwarz, S. *Chem. Commun.* **1999**, 121−122. (c) Capel-Sanchez, M. C.; Campos-Martin, J. M.; Fierro, J. L. G.; de Frutos, M. P.; Padilla Polo, A. *Chem. Commun.* **2000**, 855−856.

(23) Cotton, F. A.; Wilkinson, G. *Advanced Inorganic Chemistry*, 5th ed.; Wiley-Interscience, New York, 1988.

(24) (a) Bradley, D. C.; Gothra, J. S.; Hart, F. A.; Hursthouse, M. B.; Raithby, P. R. *J. Chem. Soc., Dalton Trans.* **1977**, 1166−1172. (b) Aspinall, H. C.; Bradley, D. C.; Sales, K. D. *J. Chem. Soc., Dalton Trans.* **1988**, 2211−2213. (c) Aspinall, H. C.; Moore, S. R.; Smith, A. K. *J. Chem. Soc., Dalton Trans.* **1992**, 153−156.

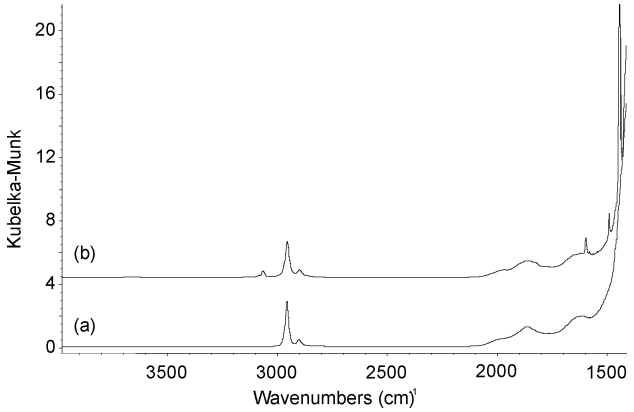

Figure 5. DRIFT spectra of (bottom) **2a** and (top) **3a**.

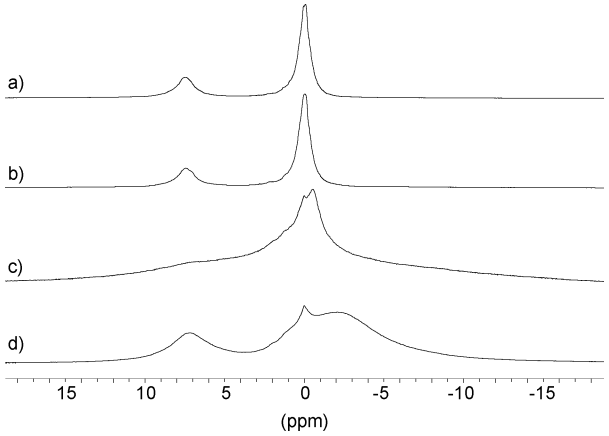

Figure 6. ^{1}H MAS spectra of (a) **3a**, (b) **3b**, (c) **3c**, and (d) **3d** (400 MHz).

indicates a certain degree of lability and therefore, to some extent, shows that triphenylphosphine oxide coordination strength can be affected by modifications within the coordination sphere. Owing to these reactivity patterns, the reaction of triphenylphosphine oxide with grafted rare-earth amides **2a**−**d** was studied. If one considers the surface as a bulky siloxide ligand, monoadducts of the type [(≡Si−O)-Ln{N(SiMe$_3$)$_2$}$_2$(O═PPh$_3$)] should be obtained, as bisadducts are expected to be far too crowded to be stable.[25] Upon exposure of toluene suspensions of **2a**−**d** with solutions containing a 3-fold excess of triphenylphosphine oxide, modified silicas **3a**−**d** were obtained. These colorless (**3a**,**b**,**d**) or light blue (**3c**) solids were washed with toluene to eliminate excess OPPh$_3$ and thoroughly dried under secondary vacuum (10^{-6} mmHg). Elemental analyses performed on **3a**−**d** indicate phosphorus/metal ratios close to 0.8 (Table 2).

These values indicate partial formation of the grafted monoadducts: Reaction with triphenylphosphine oxide affords a mixture of surface species, namely, 80% of the monoadduct [(≡Si−O)Ln{N(SiMe$_3$)$_2$}$_2$(O═PPh$_3$)] and 20% of the starting bisamido species, regardless of extended reaction times and stoichiometry (Scheme 2). Moreover, because the inorganic support is nonporous, diffusion-related limitations can be excluded.

b. DRIFTS Studies on 3a−**d.** DRIFT spectra for samples **3a**−**d** (Figure 5) show new bands corresponding to sp^2 C−H stretching (3066 cm^{-1}) and aromatic C−C bond deformations (1593, 1577, 1487, and 1440 cm^{-1}). Slight modifications in the region of sp^3 C−H elongation vibrations are observed, namely, an intensity decrease of the shoulder located at lower wavenumbers (around 2900 cm^{-1}). The O═P band, expected in the 1180−1120 cm^{-1} range, could not be detected.[24,26]

c. MAS NMR Studies on 3a−**d**. ^{1}H, ^{13}C, and ^{31}P NMR MAS spectra confirm the presence of coordinated O═PPh$_3$. Proton NMR spectroscopy reveals, for diamagnetic species **3a** and **3b**, the presence of both aromatic (7.43 and 7.41 ppm, respectively) and trimethylsilyl protons (−0.10 and −0.02 ppm, respectively) (Figure 6). On the other hand, as observed for their parent grafted amido species **2c** and **2d**, materials containing paramagnetic species **3c** and **3d** display signals outside the classical spectral window. Neodymium derivative **3c**, in addition to the surface-bound SiMe$_3$ peak (0.03 ppm), displays two major peaks, at −0.54 and 7.5 ppm, the latter of which is broader (Figure 6). In the high-field region, the spectrum comprises a shoulder that, on the basis of elemental analysis data, can be assigned to unreacted monosiloxybisamido neodymium surface species (−7.1 ppm). Similarly, in addition to the O−SiMe$_3$ signal (0.00 ppm), the spectrum of the samarium analogue **3d** comprises two peaks, at 7.20 and −2.10 ppm, the latter value being close to the chemical shift of the Sm−N(SiMe$_3$)$_2$ protons at −2.60 ppm in **2d**.

The coordination of O═PPh$_3$ to lanthanide amido species was confirmed by analysis of the 2-dimensional ^{1}H−^{1}H double-quanta correlation spectrum of 3b (Figure 7), which shows a strong correlation between aromatic and trimethylsilyl protons. This technique, called DQ-MAS,[27] was introduced to probe the through-space proximity between nuclei of the same type, using the homonuclear dipolar interaction. This through-space dipolar interaction is characteristic of a short distance between the two types of protons, which originates from the coordination of the amido and phosphine oxide groups on the same lanthanide center. A noncorrelating peak is observed at 1.3 ppm that most probably results from traces of residual silanols.

The ^{31}P MAS spectra of diamagnetic materials **3a** and **3b** are rather similar; they consist of singlets at 39.9 ($\Delta\nu_{1/2}$ = 1200 Hz) and 39.1 ppm ($\Delta\nu_{1/2}$ = 1120 Hz), respectively (Figure 8). These chemical shift values are closely related to those of the related species [Ln{N(SiMe$_3$)$_2$}$_3$(O═PPh$_3$)] in solution: 38 ppm for the yttrium derivative and 39 ppm for the lanthanum compound.[24c] The ^2J_Y−P coupling, expected to be ca. 9−14 Hz, is not observed because of the broadening of the signal in the solid state.[28] The spectrum of paramagnetic **3d** is slightly different: It consists of a more

(25) [Ln{N(SiMe$_3$)$_2$}$_3$] bis-adducts of the less-crowded trimethylphosphine oxide have been reported and are described as unstable compounds: Bradley, D. C.; Gao, Y. C. *Polyhedron* **1982**, *1*, 307−310.

(26) Nakamoto, K. *Infrared Spectra of Inorganic and Coordination Compounds*; Wiley-Interscience, New York, 1970.

(27) Schnell, I.; Brown, S. P.; Low, H. Y.; Ishida, H.; Spiess, H. W. *J. Am. Chem. Soc.* **1998**, *120*, 11784−11795.

(28) Hill, N. J.; Levason, W.; Popham, M. C.; Reid, G.; Webster, M. *Polyhedron* **2002**, *21*, 445−455.

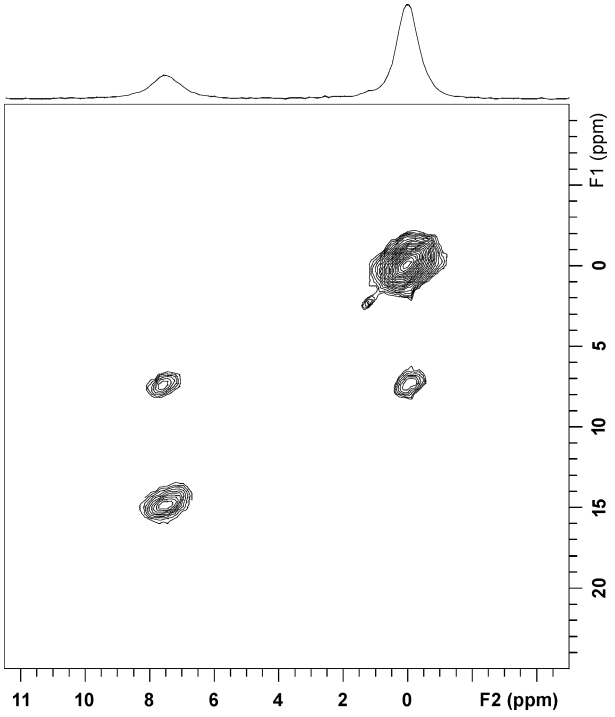

Figure 7. Double-quanta 2-dimensional $^{1}H-^{1}H$ correlation spectrum of **3b**.

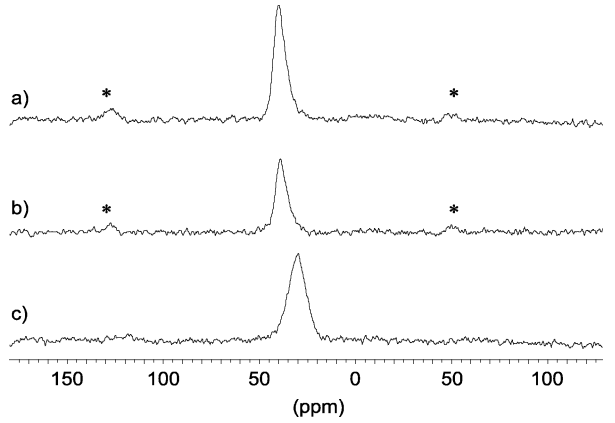

Figure 8. ^{31}P MAS spectra of (a) **3a**, (b) **3b**, and (c) **3d** (162 MHz).* = spinning side bands.

shielded and broader singlet centered at 29.6 ppm ($\Delta\nu_{1/2}$ = 1800 Hz) (Figure 8). As a comparison, physisorbed triphenylphosphine oxide gives rise to a peak at 30.3 ppm, with a width at half-height of 1450 Hz. It is noteworthy that no ^{31}P signal could be detected for **3c**, most probably because of the paramagnetic character of neodymium.

The ^{13}C CP-MAS spectrum of **3b** displays two peaks for the aromatic carbons (132.5 and 128.4) and one unresolved peak for the $SiMe_3$ carbons (3.75 ppm). As a comparison, the ^{13}C NMR spectrum of **2b** comprises a single signal centered at 2.30 ppm. These assignments were confirmed by a HETCOR $^{1}H-^{13}C$ correlation spectrum (see Supporting Information), where the aromatic protons (7.41 ppm) correlate with the carbons resonating at low fields (132.5 and 128.4 ppm), whereas the $SiMe_3$ protons correlate with the ^{13}C signal centered at 3.75 ppm.

d. Discussion. Similar to what is observed for their molecular counterparts, triphenylphosphine oxide coordinates to grafted rare-earth amides **2a**−**d**, affording surface adducts as evidenced by DQ-MAS NMR spectroscopy. Phosphine oxides have been used to probe the acidity of solids: As shown by Drago and co-workers, a positive ^{31}P NMR chemical shift difference ($\Delta\delta$) between physisorbed and chemisorbed OPR_3 is indicative of coordination to an acidic site, and the magnitude of the difference is correlated to the strength of the interaction.[29] Indeed, the calculated $\Delta\delta$ values for the diamagnetic samples **3a** and **3b**, 11.7 and 10.9 ppm, respectively, are in agreement with the coordination of the phosphine oxide to the Lewis acidic rare-earth metals. The observed order, with **3a** being more acidic than **3b**, is consistent with the relative Lewis acidity of the corresponding metals.

It is noteworthy that the $OPPh_3$ complexation reaction does not proceed to completion, as about 20% of these surface species do not form the expected adduct. Within the coordination sphere of the bisamido species, the metal undoubtedly relieves its coordinative and electronic unsaturation through interaction with surface siloxane oxygens; such behavior is known for surface organometallic compounds and for homogeneous (potential) models of lanthanide-grafted species.[30] In light of the observed reactivity pattern, the strength of this interaction is not uniform among the bisamido lanthanide surface species, because, in some instances, triphenylphosphine oxide does not form stable surface adducts. A major portion (about 80%) of the grafted metals in **2a**−**d** form stable adducts, whereas in a minor fraction (about 20%), the "external ligand"-free structure is thermodynamically more stable. This might be due to strong Ln−support interactions (chelating effect) or to destabilizing steric pressure in the hypothetical $OPPh_3$ adducts.

3. Compared Catalytic Studies Using Molecular (1a−**d) and Grafted (2a**−**d) Rare-Earth Amides. a. Alkene Hydrosilylation.** Rare-earth lanthanide hydride and alkyl complexes are known to efficiently catalyze the hydrosilylation of alkenes.[31] However, it has recently been shown that the much less air- and moisture-sensitive amido derivatives can also mediate this reaction. [32] More particularly, Livinghouse and Horino have demonstrated that lanthanum complex **1b** behaves as a highly efficient catalyst for the hydrosily-

(29) (a) Ossegovic, J. P.; Drago, R. *J. Catal.* **1999**, *182*, 1−4. (b) Ossegovic, J. P.; Drago, R. *J. Phys Chem. B* **2000**, *104*, 147−154.
(30) (a) Hermann, W.; Anwander, R.; Dufaud, V.; Scherer, W. *Angew. Chem., Int. Ed. Engl.* **1994**, *33*, 1285−1286. (b) Annand, J.; Aspinall, H. C.; Steiner, A. *Inorg. Chem.* **1999**, *38*, 3941−3943. (c) Annand, J.; Aspinall, H. C. *J. Chem. Soc., Dalton Trans.* **2000**, 1867−1871. (d) Lorenz, V.; Giessmann, S.; Gun'ko, Y. K.; Fischer, A. K.; Gilje, J. W.; Edelmann, F. *Angew. Chem., Int. Ed.* **2004**, *43*, 4603−4606. (e) Fischbach, A.; Kimpel, M. G.; Widenmeyer, M.; Hertdtweck, E.; Scherer, W.; Anwander, R. *Angew. Chem., Int. Ed.* **2004**, *43*, 2234−2239. (f) Nishiura, M.; Hou, Z.; Wakatsuki, Y. *Organometallics* **2004**, *23*, 1359−1368. (g) Elvidge, B. R.; Arndt, S.; Spaniol, T. P.; Okuda, J. *Dalton Trans.* **2006**, 890−901.
(31) (a) Sakakura, T.; Lautenschlager, H.-J.; Tanaka, M. *J. Chem. Soc., Chem. Commun.* **1991**, 40−41. (b) Fu, P.-F.; Brard, L.; Li, Y.; Marks, T. J. *J. Am. Chem. Soc.* **1995**, *117*, 7157−7168. (c) Voskoboynikov, Shestakova, A. K.; Beletskaya, I. P. *Organometallics* **2001**, *20*, 2794−2801. (d) Hou, Z.; Zhang, Y.; Tardif, O.; Wakatsuki, Y. *J. Am. Chem. Soc.* **2001**, *123*, 9216−9217. (e) Trifonov, A. A.; Spaniol, T.; Okuda, J. *Dalton Trans.* **2004**, 2245−2250.
(32) (a) Horino, Y.; Livinghouse, T. *Organometallics* **2004**, *23*, 12−14. (b) Rastätter, M.; Zulys, A.; Roesky, P. W. *Chem. Commun.* **2006**, 874−876.

Scheme 3. Catalytic Alkene Hydrosilylation

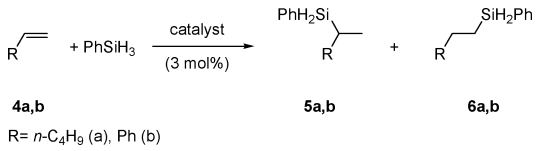

Table 3. Alkene Hydrosilylation Results[a]

run	catalyst	substrate	yield (%)	**regioselectivity (5:6)**
1	1a	**4a**	0[b]	–
2	1b		99[b]	3:97
3	1c		7[b]	4:96
4	1d		99[b]	3:97
5	2a		7[b]	nd
6	2b		98[b]	8:92
7	2b		52[c]	7:93
8	2c		85[b]	10:90
9	2c		40[c]	9:91
10	2d		82[b]	6:94
11	1a	**4b**	0[d]	–
12	1b		99[d]	>99:1
13	1c		28[d]	99:1
14	1d		99[d]	98:2
15	2a		0[d]	–
16	2b		17[d]	>99:1
17	2c		3[d]	>99:1
18	2d		1[d]	>99:1
19	2a		<1[c]	nd
20	2b		79[c]	>99:1
21	2c		28[c]	>99:1
22	2d		7[c]	>99:1

[a] Conditions: 0.03 mmol of Ln, 1 mmol of alkene, 1.1 mmol of $PhSiH_3$, 5 mL of toluene. [b] 15 h, 60 °C. [c] 5 h, 60 °C. [d] 5 h, 25 °C.

lation of alkenes and dienes with $PhSiH_3$. To evaluate the impact of the grafting of amido species **1a**−**d**, we studied the reactivity of materials **2a**−**d** in the benchmark reactions of 1-hexene (**4a**) and styrene (**4b**) with phenylsilane (Scheme 3, Table 3).

The supported lanthanide amides **2b**−**d** proved to be effective catalysts for 1-alkene hydrosilylation, whereas the yttrium-based material displays poor reactivity for this transformation, in agreement with Livinghouse et al.'s observations regarding the reactivity of **1a**. Comparison of the catalytic performances of the amides **1a**−**d** with those of the supported amides **2a**−**d** shows that, globally, if molecular (soluble) catalysts are more active than heterogeneous ones, the latter are nevertheless able to perform the same transformation with good to high yield and good to excellent selectivity. Moreover, a marked difference in substrate scale of reactivity is observed. Indeed, whereas homogeneous **1b**−**d** are significantly more reactive toward styrene than toward 1-hexene,[32a] the grafted rare-earth amides **2b**−**d** display a more balanced reactivity pattern: Under similar reaction conditions (5 h, 60 °C), the yield is only about 1.7 times higher in the lanthanum case for styrene than for 1-hexene (runs 7 and 20), and it is higher for 1-hexene than for styrene in neodymium-catalyzed hydrosilylation (runs 9 and 21). Another difference induced by the grafting lies in the metal dependence of the reactivities of the homogeneous and heterogeneous systems: Under our conditions, the reactivity order is La ≥ Sm > Nd ≫ Y for $[Ln\{N(SiMe_3)_2\}_3]$ (**1a**−**d**) and La > Nd > Sm > Y for $[(\equiv Si-O)Ln\{N(SiMe_3)_2\}_2]$ (**2a**−**d**). Thus, for grafted species, the yield increases with the Ln^{3+} ionic radius (runs 5, 6, 8, and 9; runs 7 and 9; runs 15−18; and runs 19−22), as in the case of rare-earth metallocenes.[31b,c] These tendencies (different substrate sensitivity and different metal dependence for homogeneous and heterogeneous systems) are illustrated by the fact that higher activities are obtained with grafted yttrium and neodymium amide (**2a**, run 5, and **2c**, run 8, respectively) than with the corresponding trisamides (**1a**, run 1, and **1c**, run 3, respectively).

Two factors might contribute to these differences. It has been established that the catalytically active species for this reaction is a rare-earth hydride.[31b] In the case of the amido species as catalyst precursors, initiation of the system (generation of the active species) proceeds through an amide−hydride exchange reaction: The $Ln-NR_2$ moiety reacts with phenylsilane to generate a hydride functionality Ln−H and $PhSiH_2NR_2$ as a byproduct. Indeed, when performing the hydrosilylation with homogeneous and heterogeneous catalytic systems in deuterated benzene, we observed the formation of $N(SiMe_3)_2(SiH_2Ph)$ by ^1H NMR spectroscopy.[33] Efficiency of initiation is affected by the grafting, as $N(SiMe_3)_2(SiH_2Ph)$ has been observed during 1-hexene hydrosilylation catalyzed by **2a** in C_6D_6 and not when the reaction was attempted in the presence of **1a**. This might be due to electronic changes induced by the substitution of one amido ligand in **1a**−**d** by an electron-poor siloxide in **2a**−**d**. Moreover, with the trisamides **1a**−**d**, it is likely that the generation of hydride species is followed by the formation of polynuclear compounds, examples of which have been shown to be catalysts or catalyst precursors.[31c,d] In the case of the supported catalysts **2a**−**d**, grafting of the metal onto the silica surface by a covalent bond enforces the mononuclearity of the surface hydride. As shown by Voskoboynikov and co-workers, mononuclear lanthanocene complexes are better catalysts than their dimeric counterpart for the hydrosilylation of 1-octene.[31c] This might explain why, in some instances, e.g., with Nd and Y, better activities are observed with the grafted catalyst than with the homogeneous one. In these cases, the expected higher activity of a mononuclear surface hydride species could counterbalance detrimental phenomena such as limited (hindered) substrate access to the supported catalytic site. Regarding the reactivity difference between 1-hexene and styrene, it might be that, in the surface-supported system, high electrophilicity of the metal center can be compensated by strong interactions with aryl groups or arene compounds[31b,34] which could prevent efficient ligand exchange for productive hydrosilylation. Further studies would be necessary to clarify these points.

b. Phenylacetylene Dimerization. Terminal alkyne dimerization into disubstituted 1-buten-3-ynes, as exemplified in Scheme 4 for phenylacetylene (**7**), can yield several isomers, which motivates the development of selective systems. Although this reaction can be catalyzed by rare-earth alkyl

(33) Characteristic singlet at 5.14 ppm: Mitzel, N. W.; Schier, A.; Beruda, H.; Schmidbaur, H. *Chem. Ber.* **1992**, *125*, 1053−1059.
(34) Bochkarev, M. N. *Chem. Rev.* **2002**, *102*, 2089−2118.

Scheme 4. Catalytic Dimerization of Phenylacetylene (**7**)

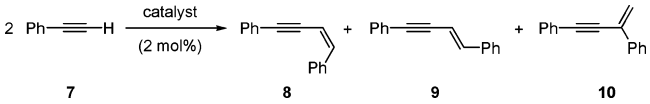

Table 4. Phenylacetylene Dimerization Results[a]

run	catalyst	conversion (%)	dimerization (%)	**8**:**9**:**10**
1	**1a**	>99	24	3:3:94
2	**1b**	99	19	41:23:36
3	**1c**	99	18	11:9:80
4	**1d**	99	33	8:39:53
5	**2a**	24	1	75:15:10
6	**2b**	75	48	41:57:2
7	**2c**	76	27	24:70:6
8	**2d**	24	11	32:62:7

[a] Conditions: 28.0 μmol of Ln, 1.34 mmol of phenylacetylene, 5 mL of toluene, 100 °C, 15 h.

derivatives,[35] Takaki and co-workers have shown that the trisamide complex **1a** combined with an amine additive (typically, $ArNH_2$ compounds) affords a catalytic precursor for the selective dimerization of **7** into **8**.[36] By drawing an analogy with surface silanols (≡Si—OH), the importance of the protic $ArNH_2$ additive in this system has encouraged us to study the influence of the grafting on the catalytic performances in the catalytic dimerization of **7** by rare-earth amides

Table 4 gathers the results obtained with the trisamides **1a**−**d** (runs 1−4) and the supported catalysts **2a**−**d** (runs 5−8). The discrepancy between the conversion of phenylacetylene and the dimerization yield is due to the formation of trimers and higher oligomers. Better selectivity toward dimerization is obtained with the supported lanthanum and neodymium catalysts (runs 6 and 7), compared to **1b** and **1c** (runs 2 and 3), in the absence of any additive to the catalytic systems. On the other hand, the yttrium- and samarium-based materials display lower activities than the corresponding amido complexes. The selectivity in the formation of the differents isomers changes significantly upon grafting of the metal center: Whereas significant amounts of **10** are obtained with homogeneous catalysts, the proportion of **8** and **9** is higher in the case of the grafted catalysts. However, no highly selective system emerges from the grafting, and further tuning of the catalytic system would be necessary to achieve this goal.

Conclusion

In summary, we have shown that rare-earth silylamides can be selectively grafted onto dehydroxylated silica, affording singly surface-bonded species [(≡Si—O)Ln-$\{N(SiMe_3)_2\}_2$] devoid of other organic co-ligand. This approach proved to be effective for derivatives containing yttrium, lanthanum, neodymium, and samarium, all of which are catalytically relevant metals. These surface species react with triphenylphosphine oxide to afford the [(≡Si—O)Ln-$\{N(SiMe_3)_2\}_2(O{=}PPh_3)$] surface adduct as a major (80%) species, along with unreacted siloxide bisamido species (20%). This reactivity pattern emphasizes the role of the silica support, in which neighboring surface siloxane groups can act as donating ligands and affect the chemistry of these highly oxophilic metal centers. The grafted amides proved to be catalytically active in alkene hydrosilylation and in phenylacetylene dimerization. Compared to the parent molecular rare-earth trisamides [Ln$\{N(SiMe_3)_2\}_3$] (**1a**−**d**), the supported species [(≡Si—O)Ln$\{N(SiMe_3)_2\}_2$] (**2a**−**d**) display significantly different behavior in these catalytic reactions, in some instances affording better performances than the analogous homogeneous systems in terms of activity and selectivity. Because immobilization on the silica surface leads to a single type of grafted species, controlled modification of the grafted metal's ligand sphere, as in molecular chemistry, can lead to the development of more efficient rare-earth-based catalytic systems.

Acknowledgment. This article is dedicated to the memory of John A. Osborn and Jacky Kress. We thank the CNRS and the Ministère de l'Education Nationale et de la Recherche for their financial support, Bertrand Revel and Catherine Méliet for NMR measurements, and Dr. Christophe Dujardin for his assistance with DRIFT spectroscopy. Dr. Prashant Deshmukh is acknowlegded for his kind help with the manuscript's proof-reading. Prof. W. Evans is thanked for helpful discussions.

Supporting Information Available: HETCOR $^1H-^{13}C$ correlation spectrum of **3b**. This material is available free of charge via the Internet at http://pubs.acs.org.

IC0610334

(35) (a) den Haan, K. H.; Wielstra, Y.; Teuben, J. H. *Organometallics* **1987**, *6*, 2053−2060. (b) Heeres, H. J.; Teuben, J. H. *Organometallics* **1991**, *10*, 1980−1986. (c) Duchateau, R.; van Wee, C. T.; Teuben, J. H. *Organometallics* **1996**, *15*, 2291−2302. (d) Nishiura, M.; Hou, Z.; Wakatsuki, Y.; Yamaki, T.; Miyamoto, T. *J. Am. Chem. Soc.* **2003**, *125*, 1184−1185. (e) Tazelaar, C. G. J.; Bambirra, S.; van Leusen, D.; Meetsma, A.; Hessen, B.; Teuben, J. H. *Organometallics* **2004**, *23*, 936−939.

(36) (a) Komeyama, K.; Takehira, K.; Takaki, K. *Synthesis* **2004**, 1062−1066. (b) Komeyama, K.; Kawabata, T.; Takehira, K.; Takaki, K. *J. Org. Chem.* **2005**, *70*, 7260−7262.